*Transactions of the Materials Research Society of Japan* 29[4] 1101-1104 (2004)

# Preparation of Ferroelectric $PbSc_{0.5}Ta_{0.5}O_3$ Thin Films by Pulsed Laser Deposition

Shuichi Murakami, Daniel Popovici*, Kazuo Satoh, Koji Inoue, Minoru Noda* and Masanori Okuyama*
Technology Research Institute of Osaka Prefecture, 2-7-1 Ayumino Izumi, Osaka 594-1157
Fax: +81-725-51-2699, e-mail: sh-murakami@tri.pref.osaka.jp
*Osaka University, 1-3 Machikaneyama-cho, Toyonaka, Osaka 560-8531
Fax: +81-6-6850-6341, e-mail: popovici@semi.ee.es.osaka-u.ac.jp

Solid solution $PbSc_{0.5}Ta_{0.5}O_3$ (PST) ferroelectric thin films have been prepared on $Pt/Ti/SiO_2/Si$ substrate by Pulsed Laser Deposition method. As-deposited PST thin film, prepared at 400 °C with $O_2$ pressure of 27 Pa, has a perovskite phase and a preferred orientation with (222) dominant. The PST thin film, post-annealed at 500 °C in flowing oxygen, shows an improved ferroelectricity compared to the as-deposited PST thin film, where the polarization at zero electric field is 1.4 $\mu C/cm^2$. The dielectric constant is 70 at 25 °C and decreases monotonically with increasing temperature ranging from 20 to 50 °C, indicating that Curie temperature is below 20 ℃. The Temperature Coefficient of Dielectric constant (TCD) is as high as 0.94 %/K at 25 °C. This means that the PST thin film is a promising candidate material for use in the infrared image sensor of dielectric bolometer mode which is based on the temperature dependence of dielectric constant.

Key words: $PbSc_{0.5}Ta_{0.5}O_3$, ferroelectric thin film, pulsed laser deposition, infrared sensor

## 1. INTRODUCTION

Recently, considerable attention has been directed toward uncooled thermal-type infrared (IR) sensor of dielectric bolometer (DB) mode [1,2,3]. This arises from the fact that it has high sensitivity, chopperless, low-power and room-temperature operation. In the IR sensor of DB mode, the dielectric constant change against temperature is detected after IR absorption through the capacitance change in the thin ferroelectric film such as $(Ba_{1-x}Sr_x)TiO_3$ (BST) [4,5], $Ba(Ti_{1-x}Sn_x)O_3$ (BTS) [6,7], $Pb(Mg_{1-x}Nb_x)O_3$-$PbTiO_3$ (PMN-PT) and $(Sr_{1-x}Ba_x)Nb_2O_6$ (SBN) [8]. In order to obtain the high figure-of-merit such as voltage responsivity ($R_v$) and specific detectivity ($D^*$), it is advantageous for the ferroelectric thin film to have Curie temperature ($T_c$) close to the operating temperature.

We have so far reported on the IR sensor of DB mode with the BST and BTS films as an IR detecting ferroelectric material, where the high figure-of-merit were obtained, and some 2-D array sensors were demonstrated [4-8]. However, the BST film having high sensitivity showed low resistivity and the film having high insulation showed low sensitivity. So, it was difficult to obtain good performance with high reliability, reproducibility and stability.

Solid solution $Pb(Sc_{0.5}Ta_{0.5})O_3$ (PST) in the complex perovskite structure ($A(B'B'')O_3$) is another attractive candidate material for the IR sensor of DB mode. Since fully B-site-cation-ordered PST exhibits a first order phase transition over the temperature range of 0 to 26 ℃ [9], the PST thin film is expected to show a high temperature coefficient of dielectric constant (TCD) around room temperature. The PST films have been grown by sputtering [10,11], sol-gel [12], metal-organic chemical vapor deposition [13] and pulsed laser deposition (PLD) [14]. However, there have been few reports concerning the PST deposition on $Pt/Ti/SiO_2/Si$ substrate, on which we have previously developed a monolithic integration of a detecting capacitor, signal-processing MOSFETs and thermally insulated structure for detector pixel by using Si-bulk-micromachining process [15].

In this paper, PST films are prepared by PLD. It is found that the PST film shows ferroelectricity, high TCD and simultaneously low dielectric loss, suggesting that the film is a promising candidate material for the IR sensor of DB mode.

## 2. EXPERIMENT

Hot pressed PST target with 20 wt% excess PbO by TOSHIMA MFG CO., LTD. was used to prepare the PST films. Deposition and annealing conditions are shown in Table I. The PST films were deposited by ArF excimer laser ablation (wavelength 193 nm and repetition rate 5Hz). Laser energy density was set at 1.5 $J/cm^2$ at the target. The substrate was held at temperatures of 300 to 600 ℃, and $O_2$ pressure was kept at 27 Pa during the film deposition. The distance from the target to the substrate was 30 mm. The deposition was performed for 4 h, and the film thickness was 300 nm. The films were post-annealed for 30 min with temperature range of 400 to 800 ℃ in flowing oxygen.

The substrate was $Pt/Ti/SiO_2/Si(100)$. Metal layers (20 nm Ti and 200 nm Pt) were successively deposited by RF magnetron sputtering on thermally oxidized

Table I. Conditions of deposition and post-annealing of PST films by PLD.

| | |
|---|---|
| Target | PST ceramic disk |
| Substrate | $Pt/Ti/SiO_2/Si(100)$ |
| Substrate temperature | 300-600 ℃ |
| Gas pressure | 27 Pa |
| Laser | ArF excimer |
| Repetition frequency | 5 Hz |
| Fluence | 1.5 J/cm$^2$ |
| Target-substrate distance | 30 mm |
| Deposition time | 4 h |
| Annealing Temperature | 400-800 ℃ |
| Annealing time | 30 min |

Si(100) wafer. In order to fabricate Metal-Ferroelectric-Metal capacitors, the top Pt electrode, 0.57 mm in diameter and 200 nm thick, was deposited on the PST films by RF magnetron sputtering.

Crystallographic orientation was analyzed by x-ray diffraction (XRD), and a scanning electron microscope (SEM) was used to observe film surface morphology. Polarization hysteresis and leakage current were evaluated by the ferroelectric test system (TOYO Corporation). Dielectric constant and loss value were measured using an LCR meter at 1 kHz and 1 V in the temperature range of 20 to 50 ℃.

## 3. RESULTS AND DISCUSSION

### 3.1 Influence of substrate temperature

Figure 1 shows the substrate temperature dependence of the XRD patterns of the as-deposited films on $Pt/Ti/SiO_2/Si(100)$. The PST film deposited at 300 ℃ has an amorphous structure. In contrast, the PST films deposited in the temperatures over 450 ℃ exhibit a predominant peak (pyr(222)) corresponding to the PST pyrochlore phase. Only the PST films deposited at 400 ℃ shows the peak (per(222)), indicating that preferential orientation is the PST perovskite (222). It is found that substrate temperature is the principle factor in obtaining a high crystalline quality with the PST perovskite (222) orientation.

In this work, we focus on the PST films deposited at 400 ℃, since it was found that the films, once deposited as the PST pyrochlore phase, were not be transformed to perovskite phase, and that the amorphous PST films deposited at 300 ℃ were prone to be transformed to the PST pyrochlore phase by post-annealing on the condition described above.

### 3.2 Influence of post-annealing

The PST films deposited at 400 ℃ exhibit a predominant PST perovskite (222) peak, but a small ferroelectricity as shown later in Fig. 3. Therefore, we investigate the post-annealing effect so as to improve the ferroelectricity. Figure 2 shows the XRD patterns of the PST films deposited at 400 ℃ before and after post-annealing at the temperature of 400 to 800 ℃. The XRD patterns show that the PST pyrochlore (222) peak intensity increases slightly as the post-annealing temperature increases. In contrast, the PST perovskite (222) peak intensities are almost the same at the post-annealing temperature range of 400 to 500 ℃, and

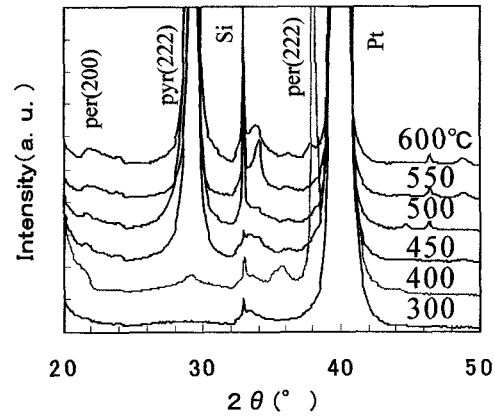


Fig. 1 XRD patterns of PST films on $Pt/Ti/SiO_2/Si$ substrate as a parameter of substrate temperature.

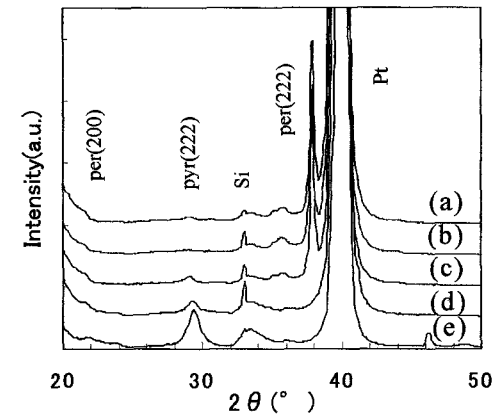


Fig.2. XRD patterns of PST films on $Pt/Ti/SiO_2/Si$ substrate as parameter of post-annealing temperature ((a) as-deposited, (b) 400, (c) 500, (d) 550, (e) 800 ℃.

the peak disappears at the post-annealing temperature above 550 ℃. It becomes clear that the PST films deposited by PLD are prone to be thermally stable in the pyrochlore phase rather than the perovskite phase.

Figure 3 shows the *P-E* hysteresis loops at room temperature of about 25 ℃ for the PST films deposited at 400 ℃ before and after post-annealing at the temperature of 400 to 550 ℃. The as-deposited PST film shows a small ferroelectricity with a polarization of 0.5 $\mu$ C/cm$^2$ at zero electric field, and the 500-℃ -annealed PST film exhibits the improved ferroelectricity with a polarization of 1.4 $\mu$ C/cm$^2$ at zero electric field, which is three times as large as that of the as-deposited PST films.

On the other hand, the PST films, which are annealed above 550 ℃, show almost no ferroelectricity. This phenomenon is consistent with the experimental result that the 550-℃-annealed PST film does not show the PST perovskite (222) peak as seen in Fig. 2.

It is interesting to note that the ferroelectricity of the PST film was improved by post-annealing at 400 and 500 ℃, whereas the PST perovskite (222) peak

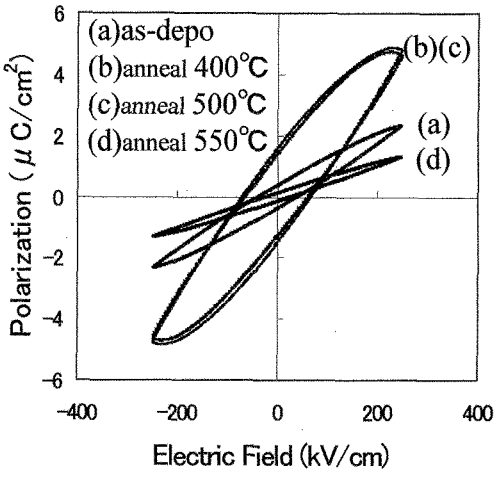


Fig. 3 P-E hysteresis loops of 400-℃-deposited PST films at different post-annealing temperatures.

intensities of the PST films are almost the same before

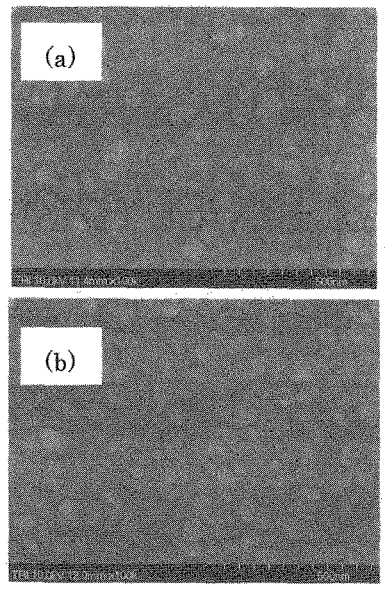


Fig. 4 SEM images of PST films before and after post-annealing at 500 ℃.

and after post-annealing. Thus, we investigate the influence of post-annealing at 500 ℃ on surface morphology, leakage characteristics and dielectric constant in order to make clear the reason for the improvement of the ferroelectricity.

Figure 4 shows SEM images of surface morphology of the PST films before and after post-annealing at 500 ℃. As seen in the figure, the both films consist of spherical grains and there are little pores between the grains. It is found that there is no considerable change before and after post-annealing. The grain size is approximately 50 nm, which is much smaller than the reported grain size of bulk PST (about 2-8 μm) [16].

Figure 5 shows current density vs. electric field at room temperature of about 25 ℃ for the PST films

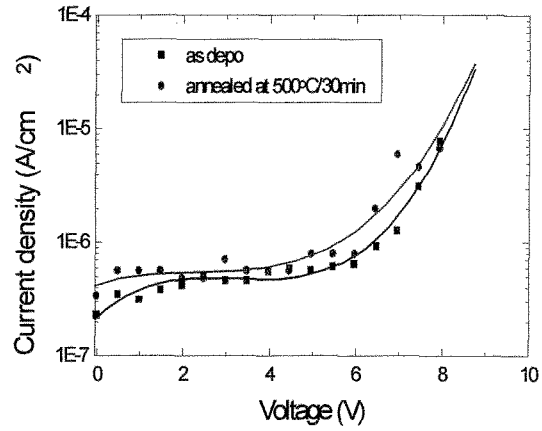


Fig. 5 Current density vs. applied voltage for PST films before and after post-annealing at 500 ℃.

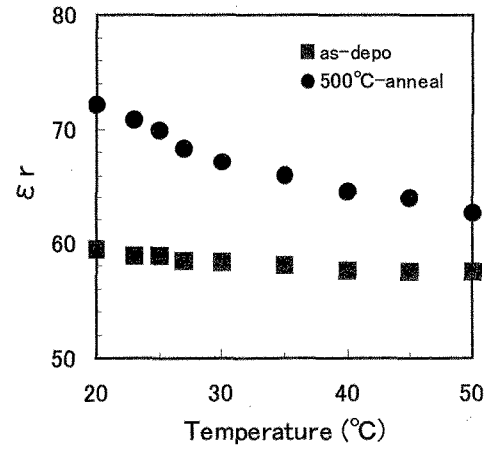


Fig. 6 Temperature dependence of dielectric constant of PST films before and after annealing at 500 ℃.

before and after post-annealing at 500 ℃. It is found from the figure that the leakage currents of the both films are relatively small and nearly the same.

Figure 6 shows the temperature dependence of the relative dielectric constant of the PST films before and after post-annealing at 500 ℃. In this figure, the dielectric constants of the both films decrease monotonically as the temperature increases, indicating that $T_c$ is below 20 ℃. This results in the P-E hysteresis loops that no saturation of the polarization was observed, as seen in Fig. 3.

The temperature dependence of the dielectric constant is relatively broad, which is different from sharp change of dielectric constant observed in bulk PST ferroelectrics [14]. This phenomenon is explained in the framework of the diffuse phase transition behavior [17]. Moreover, the relative dielectric constants of the both films are much smaller than the bulk ferroelectrics, which are considered to be due to the fact that the grain size of the films is by two orders of magnitude smaller than that of the bulk ferroelectrics [16].

Compared to the as-deposited PST film, the film after post-annealing at 500 ℃ shows clear temperature

dependence in dielectric constant. It is worth mentioning that this is consistent with the ferroelectric behavior that is improved by post-annealing as seen in Fig. 3.

From the above experimental results, it is found that the post-annealing at 500 ℃ does not affect the improvement of the crystalline property, surface morphology and leakage characteristics. However, the ferroelectric property is greatly improved, and temperature dependence of the dielectric constant becomes sharper after post-annealing. This phenomenon is considered to be due to the improvement of the domain structure, contact between the bottom electrode and the PST film or the enhancement of the degree of order for B-site cations ($Sc^{3+}$, $Ta^{5+}$) [12]. The detailed mechanism is under consideration.

3.3 Temperature coefficient of dielectric constant

In application to the infrared (IR) sensor of dielectric bolometer (DB) mode, it is important to exhibit high temperature coefficient of dielectric constant (TCD) at room temperature. TCD is expressed as

$$TCD = \frac{1}{\varepsilon_r}\frac{d\varepsilon_r}{dT} \times 100 \ (\%/K) \quad ,$$

where $\varepsilon_r$ is relative dielectric constant and $T$ is temperature. The TCDs of the PST films before and after post-annealing at 500 ℃ are determined to be 0.18 and 0.94 %/K (at 25 ℃), respectively. The TCD of the post-annealed PST film is high enough to make it possible to apply for human-detection. Furthermore, the dielectric loss was about 0.04-0.07 at 1 kHz and 1 V in the temperature range of 20 to 50 ℃. Therefore, it is concluded that the PST film is a good candidate material for the IR sensor of DB mode.

## 4. CONCLUSIONS

Solid solution $PbSc_{0.5}Ta_{0.5}O_3$ films were prepared on $Pt/Ti/SiO_2/Si(100)$ substrates by pulsed laser deposition method. It is found that substrate temperature was the principle factor in obtaining a high crystalline PST perovskite structure, and that the PST film has the preferential perovskite (222) orientation, only when deposited at 400 ℃. The ferroelectricity was improved by post-annealing at the temperature range of 400 to 500 ℃, whereas little change was observed in the crystalline property, surface morphology and leakage characteristics. It is interesting to note that the perovskite phase disappears by post-annealing above 550 ℃.

The PST film, deposited at 400 ℃ and post-annealed at 500 ℃, shows a ferroelectricity with a polarization of 1.4 $\mu$ C/cm$^2$ at zero electric field. The grain size was approximately 50 nm, and the leakage currents of the both films are relatively small. The dielectric constant decreases monotonically with increase of the temperature ranging from 20 to 50 ℃.

The TCD was determined to be 0.98 %/K at 25 ℃, implying that the film is a promising candidate material for use in the infrared sensor of dielectric mode.

## 5. REFERENCES

[1] J. F. Belcher, C. M. Hanson, H. R. Beratan, K. R. Udayakumar and K. L. Soch, *Infrared technology and Applications XXIV*, **3436**, 612-622 (1998).

[2] M. Noda, K. Hashimoto, R. Kubo, H. Tanaka, T. Mukaigawa, H. Xu and M. Okuyama, *Sensors and Actuators A*, **77**, 39-44 (1999).

[3] M. A. Todd, P. A. Manning, P. P. Donohue, A. G. Brown and R. Watton, *Infrared technology and Applications XXVI*, **4130**, 128-139 (2000).

[4] H. Zhu, M. Noda, T. Mukaigawa, H. Xu, K. Hashimoto, M. Okuyama, *T. IEEE Japan*, **120-E**, 554-558 (2000).

[5] M. Noda, K. Inoue, M. Ogura, H. Xu, S. Murakami, H. Kishihara and M. Okuyama, *Transducers '01 Munich, Germany*, 564-567 (2001).

[6] T. Miyamoto, S. Murakami, K. Inoue, Y. Suzuki, T. Nomura, M. Noda and M. Okuyama, *13th IEEE Int. Symp. on the Application of Ferroelectrics*, 191-194 (2002).

[7] M. Noda, T. Nomura, D. Popovici, Y. Kuwahara, S. Murakami and M. Okuyama, *Proc. of the 20th Sensor Symposium*, 199-204 (2003).

[8] K. Hashimoto, H. Xu, T. Mukaigawa, R. Kubo, H. Zhu, M. Noda and M. Okuyama, *Sensors and Actuators A*, **88**, 10-19 (2001).

[9] P. P. Donohue, M. A. Todd, C. J. Anthony, A. G. Brown, M. A. C. Harper and R. Watton, *Integrated Ferroelectrics*, **41**, 25-34 (2001).

[10] I. M. Reaney, D. J. Barber and R. Watton, *J. Mater. Sci.*, **3**, 51-63 (1992).

[11] M. A. Todd, P. P. Donohue, J. C. Jones, D. J. Wallis, M. J. Slater, M. A. Harper and R. Watton, *Integrated Ferroelectrics*, **25**, 113-123 (1999).

[12] D. Liu and D. A. Payne, *J. Appl. Phys.*, **77**, 3361-64 (1995).

[13] C. H. Lin, S. W. Lee and H. Chen, Appl. Phys. Lett., **75**, 2485-87 (1999).

[14] C. Bjormander, K. Sreenivas, A. M. Grishin and K. V. Rao, *Appl. Phys. Lett.*, **67**[1], 58-60 (1995).

[15] H. Xu, K. Hashimoto, T. Mukaigawa, H. Zhu. R. Kubo, T. Usuki, H. Kishihara, M. Noda, Y, Suzuki and M. Okuyama, *Infrared technology and Applications XXVI*, **4130**, 140-151 (2000).

[16] H. Wang and W. A. Schulze, *J. Am. Ceram. Soc.*, **73**[5], 1228-34 (1990).

[17] N. Setter and L. E. Cross, *J. Appl. Phys.*, **51**(8), 4356-60 (1980).

(Received October 11, 2003; Accepted March 10, 2004)